

Flight Characterization of New Generation GNSS Satellite Clocks

Montenbruck O.; *Deutsches Zentrum für Luft- und Raumfahrt (DLR/GSOC)*
Steigenberger P.; *Technische Universität München (TUM/IAPG)*
Schönemann E.; *Technische Universität Darmstadt (TUDA/IPGD)*
Hauschild A.; *Deutsches Zentrum für Luft- und Raumfahrt (DLR/GSOC)*
Hugentobler U.; *Technische Universität München (TUM/IAPG)*
Dach R.; *Astronomisches Institut der Universität Bern (AIUB)*
Becker M.; *Technische Universität Darmstadt (TUDA/IPGD)*

BIOGRAPHIES

Oliver Montenbruck is head of the GNSS Technology and Navigation Group at DLR's German Space Operations Center (GSOC). His research activities comprise spaceborne GNSS receiver technology, autonomous navigation, spacecraft formation flying, precise orbit determination and GNSS signal analysis.

Erik Schönemann is a research associate at the Institute of Physical Geodesy (IPGD) of Technische Universität Darmstadt (TUDA). His areas of research are GNSS orbit and clock determination in view of Multi-GNSS/Signal processing and the associated biases.

Peter Steigenberger works at the Institute of Astronomical and Physical Geodesy of Technische Universität München (TUM). His research interests include global GNSS solutions and the analysis of the GNSS-derived parameter time series, e.g., troposphere delays, station coordinates, satellite orbits, and Earth rotation parameters.

André Hauschild is a scientific staff member at DLR's German Space Operations Center. His work focuses on precise real-time orbit and clock estimation for GNSS satellites as well as multi-GNSS processing using modernized GPS and new satellite navigation systems.

Urs Hugentobler is full professor at the Institute of Astronomical and Physical Geodesy of Technische Universität München, and head of the Research Establishment Satellite Geodesy. His research focuses on precise GNSS applications such as positioning, orbit determination, reference frames, and time transfer.

Rolf Dach is head of the GNSS research group at the Astronomical Institute of the University of Bern (AIUB). He leads the development of the Bernese Software package and is responsible for the activities of the Center for Orbit Determination in Europe (CODE).

Matthias Becker is Full Professor of Geodesy and Director of the Institute of Physical Geodesy, Technische Universität Darmstadt. He is responsible for research and teaching in the field of Physical Geodesy and Satellite Geodesy.

ABSTRACT

The passive hydrogen maser (PHM) of GIOVE-B and the latest generation of Rubidium clocks for GPS Block IIF satellites have both demonstrated a superior and highly competitive stability in ground tests. In practice, however, the apparent clock performance for GNSS users is limited by measurement errors and imperfections of the signal chain that affect the clock variance at different time scales. Within this paper, we provide a direct comparison of the apparent clock performance for GIOVE-B and the first Block IIF satellite (SVN62). The analyses are based on observations of the IGS and CONGO network. Periodic errors in the apparent clocks of both satellites are analyzed and an effort is made to separate the impact of orbit determination errors from physical clock or line bias variations. For SVN62 an empirical clock correction model is discussed, which offers a notable reduction of the Allan variance at orbital time scales. Furthermore, triple-frequency observations are used to demonstrate the presence of thermally induced line bias variations and to quantify the resulting inter-frequency clock biases.

INTRODUCTION

The atomic frequency standard is a core component of all GNSS satellites and a high performance of the satellite clock over a wide range of time scales is desirable for multiple reasons. At time scales of 10-100 s, the clock variance directly affects the required sampling or update interval for clock solutions required by precise point positioning users. On the other extreme, a high stability at time scales of a day is of interest for the mission control segment to limit the number of broadcast ephemeris. Within the GPS constellation, the clock performance has constantly been improved with each new generation and users have taken benefit from this development through a notable reduction of the average signal in space range error ([1]-[3]).

For the European Galileo constellation, passive hydrogen masers (PHM) will be employed as primary frequency standard [4]. A first clock of this type is now in orbit for more than three years onboard the GIOVE-B test satellite (Fig. 1) and has so far demonstrated an excellent

performance. The PHM is made up of a physics package comprising the microwave cavity and the hydrogen supply assembly as well as a separate electronics package. Together, both modules exhibit a mass of 18 kg and a volume of 28 liters. The PHM served as frequency standard for the GIOVE-B navigation payload for most of the mission except for limited periods in which the backup Rubidium clock was tested.

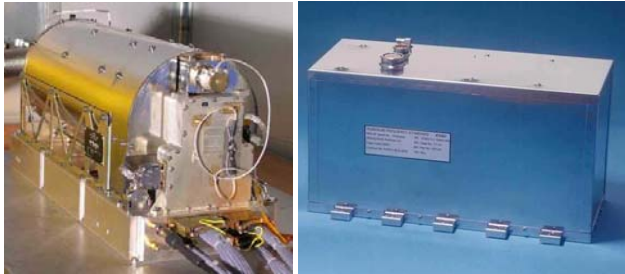


Fig. 1 GIOVE-B Passive Hydrogen Maser (*left*; credit ESA) and GPS Block IIF-1 Rubidium clock (*right*; credit Perkin-Elmer).

On GPS, a new generation of rubidium clocks (Fig. 1) has been introduced with the first Block IIF satellite (SVN62; PRN25) launched in mid 2010. It represents an advanced version of the rubidium standard in present use onboard the Block IIR satellites and benefits from various improvements in the physics package such as a Xenon buffer gas and a spectral filter for the Rb-D lines [5]. In addition, a baseplate temperature controller (BTC) has been added to effectively reduce the overall temperature sensitivity. At a volume of 2.5 liters, the new RFS-IIF rubidium frequency standard is moderately larger than the former RFS-IIR clock, but still substantially more compact than a PHM.

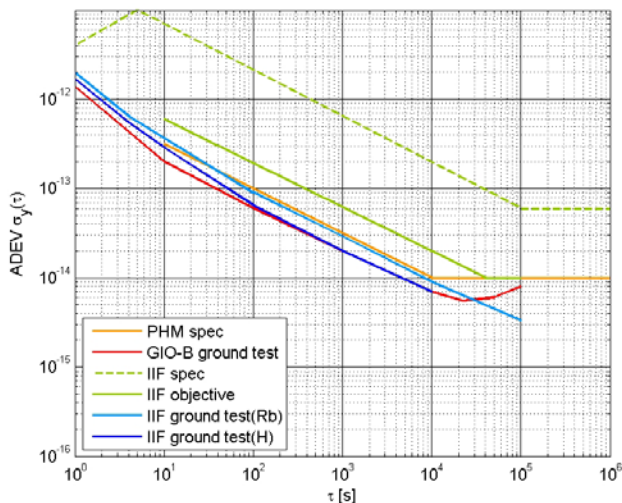


Fig. 2 Frequency stability of GIOVE-B PHM and GPS RFS-IIF clocks (ground measurements and specification).

The superior quality of both clock types is illustrated in Fig. 2. It shows the measured Allan deviations (ADEV) from ground performance tests in comparison with the respective specifications based on data published in [5]

and [6]-[8]. For the RFS-IIF clock, the targeted performance (objective) is shown in addition to the formal specification. Actual performance data are given in comparison to a Rubidium and a H-maser reference frequency standard.

The GIOVE PHM exhibits a white frequency noise of approximately $6 \cdot 10^{-13} \tau^{-1/2}$ for time intervals of 10-10,000 s, which is well within the specified range of $< 1 \cdot 10^{-12} \tau^{-1/2}$. Near 20,000 s, a flicker floor of $6 \cdot 10^{-15}$ is reached. Below 10 s, the ADEV exhibits a steeper slope close to -1 in the log-log representation, which indicates a dominating contribution of white or flicker phase noise.

For the RFS-IIF clock, a white frequency noise of less than $2 \cdot 10^{-12} \tau^{-1/2}$ is specified but a ten times better performance has been formulated as an objective [5]. In fact, the measured performance in the ground tests is in close accord with that of the GIOVE PHM. Depending on the specific device-under-test and the employed reference clock, values of $6 \cdot 10 \cdot 10^{-13} \tau^{-1/2}$ have been reported in [5] and [9].

Unfortunately, the excellent performance demonstrated in the lab environment for both the PHM and the Rb clock cannot to full extent be materialized by GNSS users of the satellites in orbit. Here, varying delays in the transmitter chain, measurement errors of the monitoring stations or imperfections of the orbit and clock determination process will affect the apparent clock observed by the user and, consequently, limit the capability to assess the actual in-orbit performance of the frequency standard itself.

For GIOVE-B, flight performance analyses of the PHM have primarily been based on ESA's GESS tracking network and the operational orbit determination and time synchronization (ODTS) process (see [8] and references therein). While a good agreement with ground test results was obtained from short arc analyses at time scales of 10-200 s, receiver noise was identified as a limiting factor at shorter intervals. On the other hand, a large bump can be observed in the Allan variance at intervals of 3,000-40,000 s which reflects a quasi-periodic clock variation at orbital period.

Similar to GIOVE-B, the rubidium frequency standard (RFS) of SVN62 shows a good stability at times scales of up to 3,000 s but exhibits an ADEV bump at longer intervals ([9], [11]). An increased clock variance due to (sub-)orbital harmonics was noted quickly after the RFS activation [11] and associated with similar variations of a geometry- and ionosphere-free triple frequency combination reported in [12].

Despite similar phenomena observed for both satellites, it is not immediately obvious whether these originate from the same cause or must be attributed to different reasons. Also, published performance results for the individual satellites are so far based on widely different tracking networks and processing tools. Within this paper, an

effort is made to provide a direct comparison of the GIOVE-B PHM and GPS Block IIF-1 RFS performance based on a joint processing of both satellites and, where feasible, common receivers. The paper starts with a discussion of the available data set and the employed processing strategies. Here, the orbit and clock determination process, the short arc clock analysis and the analysis of triple-frequency observations is addressed. Thereafter, results for the individual satellites are presented and different processing techniques are compared. Subsequently, a comparison of the overall clock performance for both satellites is provided. The paper finally discusses probable explanations for the observed long-term variance of the individual clocks.

DATA SETS AND PROCESSING

GNSS Observations

The analyses presented in this paper are based on GNSS observations from two distinct monitoring station networks with global coverage but different tracking capabilities. As part of the International GNSS Service (IGS, [13]), roughly 400 stations worldwide contribute routine observations of GPS and GLONASS satellites in the L1 and L2 frequency bands for public use. Among others, these observations provide the basis for the generation of high-quality orbit and clock products by the IGS Analysis Centers. The COoperative Network for GIOVE Observation (CONGO, [14]), in contrast, is a complementary real-time network with multi-frequency and multi-GNSS capability established by various German and international partners. Among others, CONGO supports triple-frequency (L1/L2/L5) GPS tracking, E1/E5a tracking of GIOVE-A and -B as well as L1/L2/L5 QZSS tracking. Started as an 8 station network in 2009, CONGO has expanded to 13 stations in mid 2010 and 20 stations in mid 2011 (Fig. 3). Within the context of the present study, it provides the basis for orbit and clock determination of GIOVE-B as well as the analysis of SVN62 inter-frequency biases.

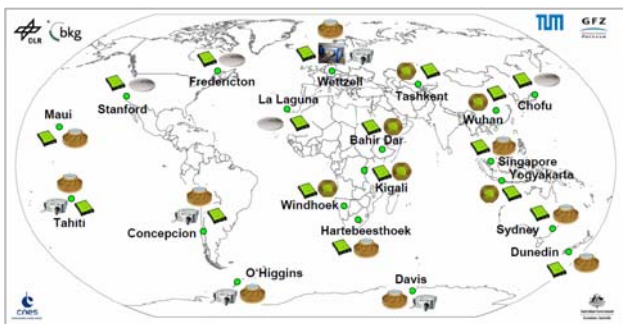


Fig. 3 CONGO network (July 2011).

Complementary to GNSS observations, laser ranging measurements collected by the International Laser Ranging Service (ILRS, [15]) have been employed for validation (and, in part, generation) of GIOVE-B orbit/clock products.

Clock Products

Along with the precise orbit determination, clock solutions for all GPS satellites are routinely generated by the IGS Analysis Centers (ACs) from a ionosphere-free combination of L1/L2 code and phase measurements. Individual AC solutions are later merged into combined clock products at 5 min or 30 s sampling. Since high-rate (30 s) clock products are only generated by a subset of IGS ACs, the resulting combination may, however, suffer from small inhomogeneities. We have therefore adopted the clock product of a single AC, namely the Center for Orbit Determination in Europe (CODE, [16]), for the analysis of the SVN62 (PRN25) clock variations. In view of a large number of tracking stations and advanced processing techniques, the GPS satellite orbits are determined with a representative accuracy of better than 2 cm [17] and a similar performance is achieved for the clock products. GPS clock products are provided on a daily basis and different reference clocks may be employed from one day to another. For the analysis of clock variations over longer time scales it is therefore necessary to realign the satellite clocks to a common reference over the entire arc. IGS sensor stations connected to hydrogen masers (such as, AMC2, HERS, ONSA, USNO, or YELL) and included in the respective clock product have been selected for this purpose. Furthermore, discontinuities at day-boundaries were removed by adding a constant daily offset to the estimated satellite-minus-station clock offset difference. Finally, a low order clock polynomial was adjusted and subtracted to obtain a detrended clock solution for computation of Allan deviations and the analysis of harmonic clock variations.

Complementary to the L1/L2 clock offset, we consider a triple-frequency combination

$$\text{DIF3}(L_1, L_2, L_5) = 0.285 \cdot L_1 - 1.546 \cdot L_2 + 1.261 \cdot L_5 \quad (1)$$

of L1, L2 and L5 carrier phase measurements in our SVN62 analysis. The geometry- and ionosphere-free linear combination represents the difference of the L1/L2 and L1/L5 ionosphere-free carrier phase combination. It matches the difference $cdt_{15} - cdt_{12}$ of clock offsets determined from L1/L5 and L1/L2 observations [18] and indicates possible inter-frequency bias variations in the respective signals. Epoch-wise estimates of the L1/L5-minus-L1/L2 clock difference for the SVN62 satellite have been obtained from triple-frequency observations of the CONGO network in a multi-day adjustment of clock differences and pass-by-pass carrier phase biases. Depending on the number of contributing stations, a representative noise level of a few mm is achieved for the estimated clock differences. Neither the triple-frequency combination (1) nor the estimated values $cdt_{15} - cdt_{12}$ depend on the clock offset itself but rather describe the inter-frequency difference of clock measurements. As such, they do not provide information on the actual reference frequency standard but enable a discrimination

of errors of the apparent clock. In particular, variations in the triple-frequency combination signify the presence of time-dependent line biases in the signal chain.

Based on observations from the CONGO network the orbit and clock offsets of GIOVE-B are routinely determined at Technische Universität München (TUM) [19]. A modified version of the Bernese software [20] is employed in this processing, which supports a wider range of observations than the standard GPS/GLONASS version. GPS orbit and clock offsets are taken from the CODE/IGS solutions and held fixed in the CONGO data processing. Here, GIOVE orbit and clock parameters are estimated along with CONGO station coordinates, clock offsets and troposphere parameters. The “final” orbit product represents the central day of a 5-day solution derived from the combination of five consecutive single-day normal solutions. Aside from the orbital elements a set of 9 solar radiation pressure (SRP) parameters are adjusted. Clock solutions are obtained at 30 s time steps consistent with the sampling of the GPS clock products.

For an independent verification of the TUM products, orbit and clock solutions of GIOVE-B have been determined for a selected one-month data arc in Aug. 2010 by Technische Universität Darmstadt (TUDA). Here, an integrated GPS/GLONASS/GIOVE processing has been performed with the NAPEOS software [21] of the European Space Agency (ESA) using both IGS and CONGO observations. The joint processing of data from all constellations and networks offers various conceptual advantages over the TUM approach, albeit at a notably increased computational burden. In particular, the estimation of site coordinates, tropospheric delays and receiver clock offsets for the CONGO stations can benefit from integer ambiguity resolution when processing these stations jointly with other IGS stations. Sliding 3-day orbit and clock solutions were generated that avoid day-boundary effects in the clock monitoring. A full set of 9 SRP model coefficients were adjusted in each processing arc. Clock offsets were computed at 30 s intervals consistent with the IGS and TUM products. While SVN62 (PRN G25) and GIOVE-B (PRN E52) clock information is jointly contained in the combined clock product of TUDA, it is obvious, though, that the corresponding information is derived from largely independent stations (IGS versus CONGO) and from observations in different frequency bands (L1/L2 versus E1/E5a). This will inevitably result in a different quality of the computed orbit and clock products, even though the estimation is strongly coupled through observations the GPS satellites that are jointly tracked by stations of both networks.

According to IGS processing conventions, a dominating relativistic correction term related to the orbital eccentricity is presently applied in the computation of satellite clock offsets from ground based GNSS measurements. However, the impact of the Earth oblateness to the gravitational potential needs to be

considered as well, when aiming at a more rigorous realization of the satellite’s proper time. The relativistic J_2 correction described in [22] has therefore been applied to all (GPS and GIOVE) clock solutions of IGS, TUM and TUDA prior to the analysis of the respective clock variances. It exhibits an amplitude of roughly 2 cm and varies with twice the argument of latitude. Consideration of the correction assists a correct interpretation of 2/rev clock variations that would otherwise be superimposed by the relativistic J_2 effect.

With the exception of CODE GPS clock products, which are also generated at 5 s intervals [23], all GNSS and reference station clock solutions products available for the present analysis are limited to a minimum sampling interval of 30 s. In order to study the satellite clock variance down to intervals of 1 Hz, we make use of a dedicated short arc analysis strategy introduced in [24]. It makes use of the fact that tropospheric delays and ephemeris errors vary slowly over time and can readily be approximated by a low order polynomial over time intervals of up to an hour. The same holds for the receiver clock offset if the receiver is connected to an ultra-stable oscillator such as a H-maser. The short term variance of the satellite clock can then be assessed by differencing the observed carrier phase against a predicted geometric range and detrending the results with a fit-polynomial. To minimize the impact of ionospheric perturbations, a ionosphere-free dual-frequency combination should be employed, but single-frequency measurements can likewise be used for short time intervals and sufficiently quiet atmospheric conditions. As pointed out in [25] the geometric range-variation can likewise be compensated by the fit polynomial, which further simplifies the analysis but potentially removes actual clock variations on the corresponding time scales. Typically the short-arc method is suitable to obtain the Allan variance at time scales of 1-100 s, which offers a sufficient overlap with the analysis of clock offsets resulting from the precise orbit and clock determination.

For the present paper, short arc analyses of the SVN62 RFS and the GIOVE-B PHM have been performed with 1 Hz observations collected at the Wettzell site of the CONGO network. Here, a Septentrio GeNeRx1, a Leica GRX1200+GNSS receiver and a Javad Delta-G3TH receiver are jointly operated from a common antenna and using a common H-maser frequency reference. To minimize the impact of thermal receiver noise, the data arcs were chosen near culmination of high elevation ($>70^\circ$) passes. When modelling the geometric range variation, a 2nd or 3rd order trend polynomial was found to be adequate for data arcs of 1 h duration.

RESULTS AND DISCUSSION

SVN62 Rubidium Frequency Standard

Following initial operations with a Caesium clock, the Rubidium clock on SVN62 was activated on 13 July 2010

and has been used as primary frequency standard since then. Only a limited number of IGS stations tracked the satellite until end of August 2010, when the spacecraft was finally set healthy, and IGS products did not yet achieve their final quality. Nevertheless, it was rapidly noted that the apparent clock of SVN62 is affected by notable periodic variations that clearly exceed the short term noise [11]. Based on a Fourier analysis, 1st, 2nd and 3rd-order harmonics of the 12h orbital period were identified in the IGS clock product [10]. In parallel, unexpected periodic variations have likewise been noted in the triple-frequency carrier phase combination [12].

By way of example, both phenomena are illustrated in Fig. 4 for a 3-day data arc during the eclipse phase in June 2011. Here, 1/rev and 2/rev variations can easily be

recognized, which exhibit a peak value of about 20 cm right after the shadow transit. The observations strongly suggest a temperature-induced effect, where positive offsets in the L1/L2 clock and the L1/L5-minus-L1/L2 clock difference correspond to a lower than average temperature of the spacecraft. Both graphs exhibit a striking similarity despite the fact that all reference frequency variations are cancelled in the triple-frequency combination. Evidently, carrier phase measurements on at least one frequency are affected by temperature-dependent line bias variations but it is not presently possible to uniquely separate such biases from possible temperature-induced variations of the rubidium clock itself [18]. Following [5], the RFS-IIR frequency standard exhibits a temperature coefficient of $\leq 2 \cdot 10^{-13}/^{\circ}\text{C}$, which is further reduced by a factor of 50 through use of the

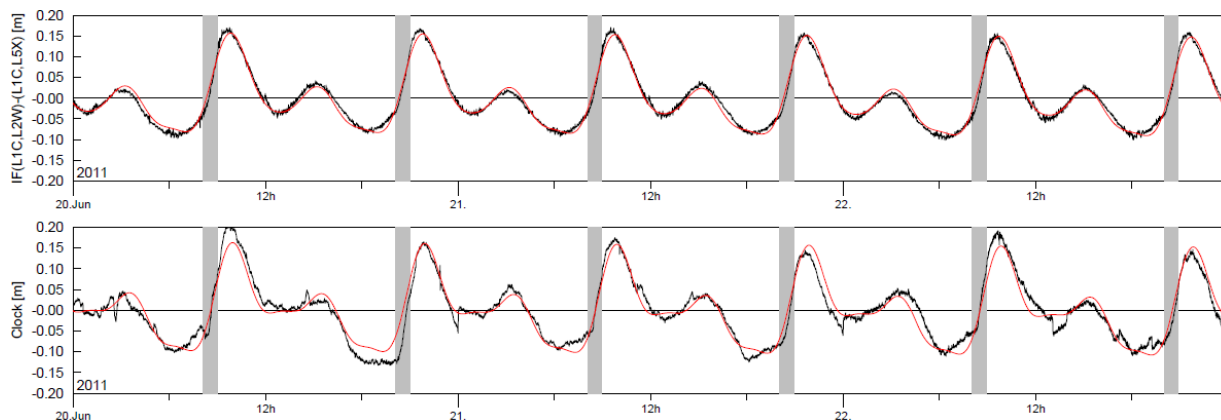


Fig. 4 Periodic variations in the detrended L1/L5-minus-L1/L2 clock difference (*top*) and L1/L2 clock solution (*bottom*) during the latest eclipse period of the Block IIF-1 (SVN62) GPS satellite. Shaded bars indicate shadow transit intervals; trendlines of a harmonic fit are shown in red.

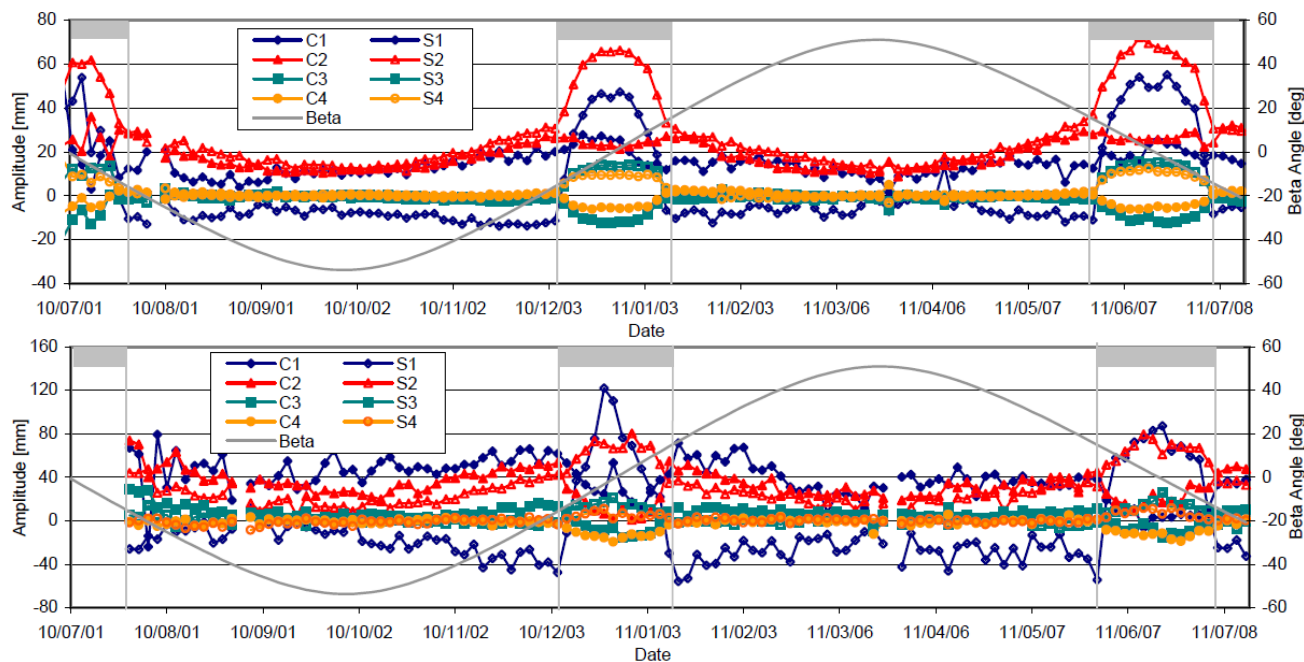


Fig. 5 Seasonal variation of harmonic coefficients for the L1/L5-minus-L1/L2 clock offset variation and the L1/L2 clock offset of the GPS Block IIF-1 satellite during the first year of operation. Eclipse periods are marked by shaded bars.

baseplate temperature controller. Measured temperature variations of 0.5°C peak-to-peak inside the Block IIF-1 spacecraft [5] would then suggest a negligible contribution of the RFS to the apparent clock variations. However, detailed spacecraft telemetry and design information is not publicly available, which inhibits a more thorough investigation.

Even without a detailed physical understanding, use can be made of the fact that the observed clock variations are strongly correlated with varying Sun illumination. More specifically, the detrended clock offset and inter-frequency clock difference can be described by a harmonic expansion

$$f(t) = \sum_{i=1}^4 [c_i \cdot \cos(i\mu) + s_i \cdot \sin(i\mu)] \quad (2)$$

in terms of the orbit angle μ which measures the in-plane position of the satellite relative to the local midnight line and is a linear function of time. The coefficients c_i and s_i obtained from a least-squares fit over consecutive 3-day data arcs throughout the first year of operation are illustrated in Fig. 5. They depend primarily on the modulus of the Sun's elevation β with respect to the orbital plane and can be approximated by a simple linear or cubic polynomial in $|\beta|$ outside and inside the eclipse period, respectively. Using a representation of the form

$$c_i = \begin{cases} c_{i,a} + c_{i,b} \cdot B^3 \\ c_{i,a} + c_{i,b} + c_{i,c} \cdot (B-1) \end{cases} \text{ for } \begin{cases} B \leq 1 \\ B > 1 \end{cases} \quad (3)$$

with $B=|\beta|/14^\circ$, the numerical vales in Table 1 have been obtained in a least squares fit of tharmonic coefficients based on one year of data. Compared to a preliminary model of this kind established in [18] from an eight months data arc, the present model offers a more compact representation and a slightly better accuracy.

Table 1 Harmonic coefficients of SVN62 L1/L2 clock offset variations.

i	c_{ia}	c_{ib}	c_{ic}	s_{ia}	s_{ib}	s_{ic}
1	10.8	40.3	-4.5	84.1	-117.8	6.6
2	8.7	42.0	-9.2	72.4	-33.2	-9.5
3	-12.1	24.2	-3.1	16.8	-17.8	0.6
4	-15.7	13.9	0.5	7.8	-7.6	-0.6

Overall, daily rms errors with a median value of less than 3 cm (0.1 ns) are achieved by the model. For comparison, a 1 cm median rms error is obtained for a corresponding representation of the L1/L5-minus-L1/L2 clock difference. Using the analytical approximation of the periodic clock errors, the clock prediction at medium to long time scales can be improved substantially, which is also reflected in a notable reduction of the Allan variance.

For a quantitative characterization of the apparent clock of SVN62, the overlapping Allan deviation (ADEV, [26]) has been computed for time intervals of 30 s to 100,000 s based on L1/L2 clock offsets estimated in the orbit and

clock determination process of CODE and TUDA. Example results are shown in Fig. 6 for a 3 days data arc in mid Aug. 2011 (DOY 225-227). For comparison, the corresponding clock variance of two IGS stations equipped with H-masers (ALGO, ONSA) is also shown. All values are referred to a common reference clock (AMC2 H-maser). Up to 2,000 s the ADEV of the apparent clock closely follows the expected $\tau^{-1/2}$ dependency, but is roughly two times larger than measured in the ground tests. At longer intervals, the 1/rev and 2/rev harmonics discussed above cause a pronounced bump with a local maximum of $4 \cdot 10^{-14}$ near 10,000 s, i.e. a quarter of the orbital period. As indicated by the grey lines, this bump can effectively be removed by applying a correction based on the model ((2)-(3)) to the observed clock. Using this correction, an Allan deviation of $1.3 \cdot 10^{-14}$ is achieved at $\tau=10,000$ s, which represents a factor of 3 performance improvement.

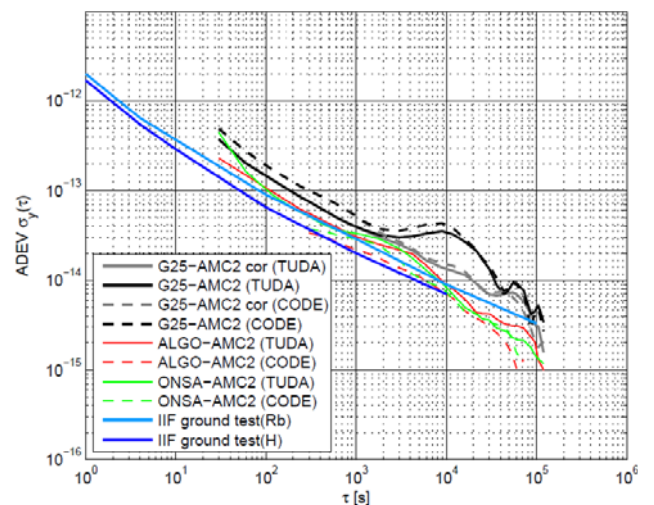


Fig. 6 Allan deviation of the SVN62 (PRN G25) Rubidium Frequency Standard and selected high-precision ground clocks as derived from the CODE and TUDA orbit and clock determination.

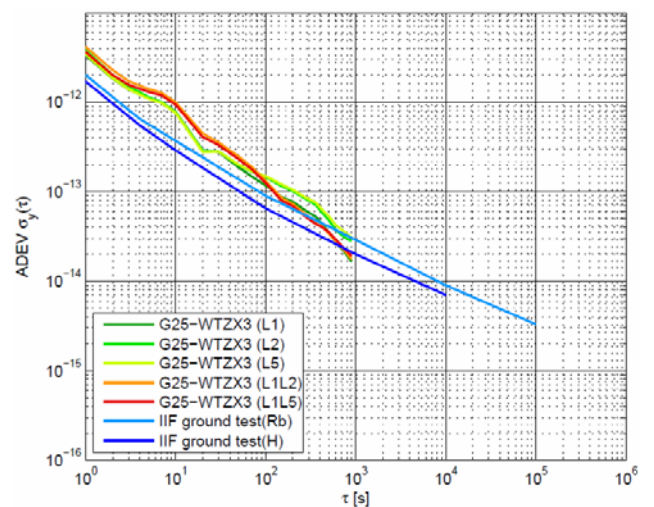


Fig. 7 Allan deviation of the SVN62 (PRN G25) Rubidium Frequency Standard from short-arc analysis of one-way carrier phase observations at the Wettzell CONGO station.

Complementary to the analysis of clock offsets from the orbit and clock determination process, the Allan variance at short times scales has been assessed based on the analysis of 1 Hz one-way carrier phase (OWCP) measurements from the Wettzell site of the CONGO network. Out of the three receivers jointly operated at this site, the WTZX3 station equipped with a Javad Delta-G3TH receiver offered the lowest noise and multipath and was therefore selected for the analysis. Results obtained for a high elevation pass on Dec 4, 2010 (DOY 339) are shown in Fig. 7.

As may be recognized, almost identical results are obtained up to about 100 s when using either single-frequency measurements or ionosphere-free dual-frequency carrier phase combinations (L1/L2 or L1/L5). Here, Allan deviations exceeding the ground test results by at most a factor of two are obtained. Apparently, receiver measurement errors, which are expected to differ by a factor of 3 for the single- and dual-frequency processing, do not impact the apparent clock estimate at short time scales and it remains unclear whether the RFS performance estimate is ultimately limited by the employed ground reference clock. A comparison of the short arc (Fig. 7) and long arc (Fig. 6) results finally shows that both methods yield a good overall consistency in the common time domain.

GIOVE-B Passive Hydrogen Maser

The use of one way pseudorange or carrier phase measurements for orbit and clock determination of GNSS satellites induces a tight coupling between orbit and clock errors. Radial orbit errors, in particular, will be reflected in almost identical clock errors due to the small off-nadir-angles of the satellite-to-station vector. While a high accuracy (~ 2 cm) is presently achieved for GPS satellites due to a very dense tracking network and the possibility to fix carrier ambiguities in the overall adjustment, the same does not presently apply to the GIOVE (Galileo) satellites.

Prior to assessing the observed performance of the GIOVE-B PHM, we therefore discuss the quality of GIOVE-B orbit determination from observations of the CONGO network. In the absence of external reference solutions from the operational GESS network of ESA, we compared the consistency of solutions obtained from a common set of CONGO observations by two independent institutions using different software packages. In addition, satellite laser ranging (SLR) measurements provided by the International Laser Ranging Service (ILRS, [15]) were used as a performance indicator. In view of systematic biases of 5-10 cm between SLR observations and GNSS based orbits of GIOVE-B that have become obvious in earlier analyses ([19], [27]), an empirical z-axis correction has been applied to the reflector position relative to the reference coordinates provided in [28]. The adopted value ($\Delta z = -7.5$ cm) was found to give a good consistency in the present analysis but is possibly uncertain to a few cm.

For the comparison, daily GNSS-only orbit products covering four weeks period in July/August 2010 from TUM (central days of 5-day arcs) and TUDA (central days of 3-day arcs) were employed. Combined GNSS-SLR solutions were, furthermore, provided by TUDA. As shown in Table 2, the individual solutions exhibit an overall consistency at the level of 10-15 cm (3D rms position difference), radial offsets of less than a few cm and a typical standard deviation of 5-10 cm in each axis.

Table 2 Inter-comparison of orbit products for DOY 208-236, 2010. Orbit differences (mean \pm std.dev.) in radial (R), transverse (T) and normal (N) direction are provided in the upper right cells, 3D rms position differences in the lower left. G and G+S denote GNSS-only and GNSS+SLR solutions. All values in m.

	TUM(G)	TUDA(G)	TUDA(G+S)
TUM(G)	-	R -0.03 \pm 0.06 T -0.03 \pm 0.09 N -0.05 \pm 0.10	R -0.03 \pm 0.08 T -0.04 \pm 0.09 N -0.01 \pm 0.08
TUDA(G)	0.15	-	R -0.01 \pm 0.03 T -0.01 \pm 0.05 N +0.04 \pm 0.08
TUDA(G+S)	0.14	0.11	-

SLR residuals statistics for the 3 types of orbit products are collated in Table 3 based on observations from northern and southern hemisphere stations of the ILRS. As expected, the smallest residuals are obtained for the GNSS+SLR solution, while biases and standard deviations of 5-10 cm are obtained for the GNSS-only solutions. Satellite laser ranging measurements of GNSS satellites are particularly sensitive to the radial position, which in turn correlates with the clock offset estimation. Accordingly, clock offset errors with a standard deviation of 5-10 cm level must be expected for the GNSS only solutions.

Table 3 Satellite laser residuals (mean \pm std.dev.) for GIOVE-B orbit products (DOY 210/217-227).

	TUM(G)	TUDA(G)	TUDA(G+S)
Residuals	6.9 \pm 7.2	+3.2 \pm 4.4	+1.0 \pm 2.8

For closer inspection, the clock offsets estimated in the three solutions are illustrated in Fig. 8 for a sample 3-day data arc (8-10 Aug. 2010) following detrending with a low order polynomial. Sinusoidal variations with 15 cm amplitude and a period of about 14 h can be recognized for the two GNSS-only solutions, but are absent or at least notably attenuated in the combined GNSS+SLR solution.

The obvious correlation of clock errors with the orbital period resembles the situation discussed earlier for the GPS SVN62 satellite and likewise suggests temperature sensitivity as a cause of the clock variations. A similar

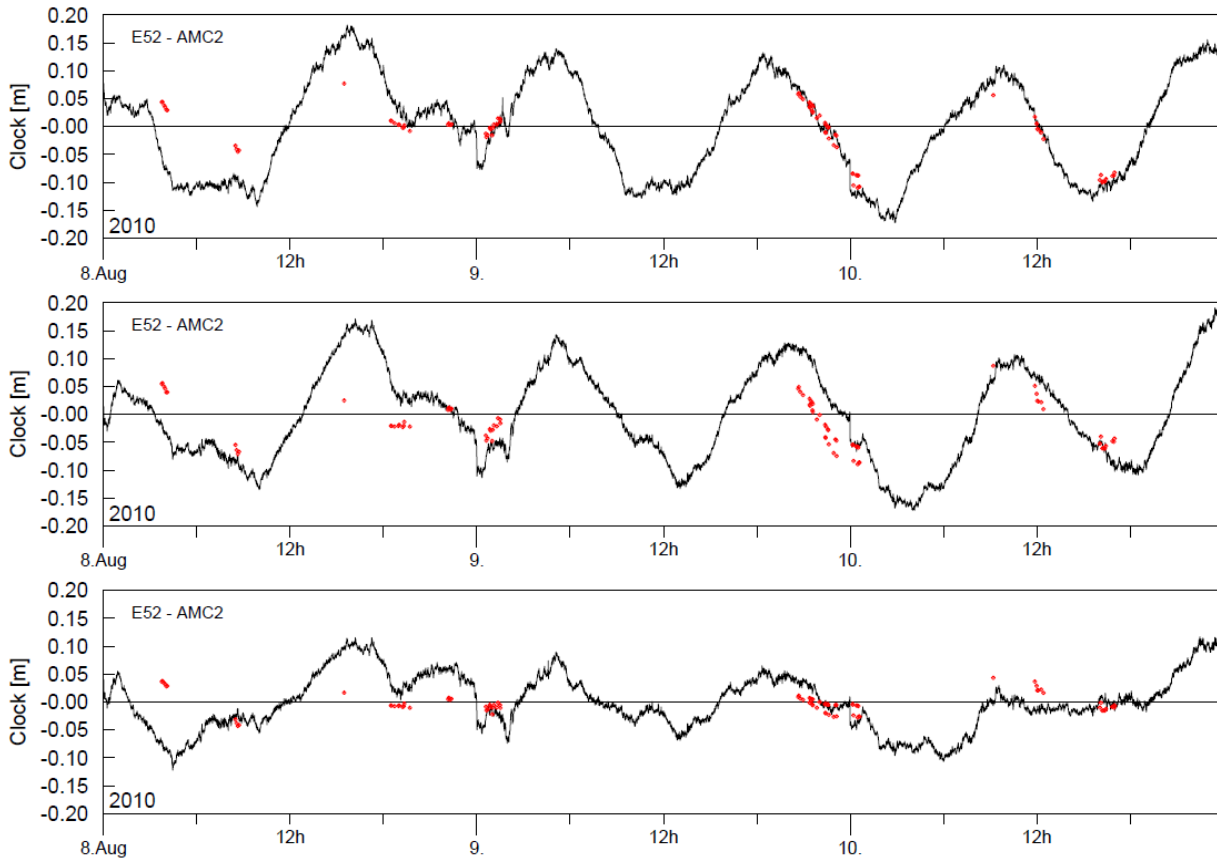


Fig. 8 Detrended GIOVE-B clock solution of TUM (GNSS-only; *top*), TUDA (GNSS-only; *center*) and TUDA (GNSS+SLR; *bottom*) for DOY 220-222, 2010. Red diamonds indicate residuals (computed-minus-observed) of satellite laser ranging measurements obtained with the corresponding orbits products.

effect has indeed been verified for the Rubidium clock of GIOVE-A, which is known to operate outside the nominal temperature range and to experience larger than planned temperature variations [6]. However, the same does not apply for the GIOVE-B PHM, which operates in a very stable thermal environment [6] and exhibits a temperature sensitivity of less than $<3 \cdot 10^{-14}/^{\circ}\text{C}$ [7]. Also, it may be noted that the thermally induced clock (or line bias) variations on SVN62 exhibit both 1/rev and 2/rev contributions of similar amplitude, whereas the apparent GIOVE-B clock variations are clearly dominated by a 1/rev periodicity.

Early evidence for orbit errors as the root cause of the GIOVE-B clock variation was given in [27]. Here, it was demonstrated that an improved consistency of adjacent orbit determination solutions can be obtained by applying a linear clock constraint in the combined orbit and clock adjustment. In parallel, Svehla et al. [29] showed that the observed GIOVE-B clock offset variations are highly correlated with the SLR residuals of the corresponding orbit solution.

The latter fact is illustrated in Fig. 8 for the three types of clock solutions discussed before. Even though the SLR tracking does not offer a continuous coverage across each

orbit, it may be recognized that the computed-minus-observed SLR residuals follow the trend of the periodic 1/rev clock offset variations in the TUM and TUDA GNSS-only solutions. For the GNSS+SLR solution, in contrast, the estimated orbit is fully consistent with the SLR observations. Here, the SLR residuals exhibit a random scatter at the level of a few cm but are essentially free of systematic variations. Evidently, the combined processing of both measurement types results in more accurate orbit estimates. In particular, it avoids errors in the orbital eccentricity that would induce radial position errors (and subsequently clock errors) with a 1/rev periodicity.

Remaining clock offset variations in the GNSS+SLR solution exhibit an amplitude of roughly 10 cm, which clearly exceeds the level of the SLR residuals but is largely free of orbit related periodicities. It is presently unclear, to what extent these variations indicate the actual long-term variance of the PHM or further network-related limitations of the clock determination process.

The benefit of the combined GNSS+SLR processing is also shown by the Allan deviation (Fig. 9) where it contributes to a notable flattening of the bump at half the orbital period. Compared to the ground test results, the

Allan deviation of the apparent clock between 30 s and 20,000 s is roughly 2-4 times larger and exhibits a slightly steeper slope than implied by a pure $\tau^{-1/2}$ dependency.

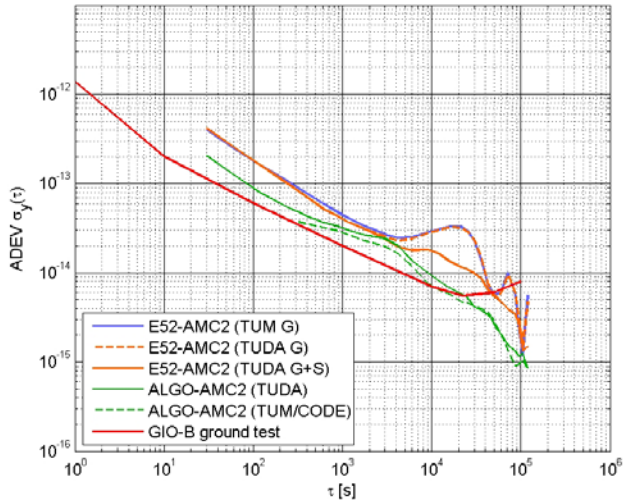


Fig. 9 Allan deviation of the GIOVE-B (PRN E52) Passive Hydrogen Maser and a high-precision ground clock as derived from the TUM/CODE and TUDA orbit and clock determination.

A similar gap between PHM lab results and in-orbit performance of the apparent clock is also obtained for the short arc ADEV analysis of one-way carrier phase measurements. Results derived from 1 Hz GIOVE-B observations with a Javad Delta-G3TH receiver during a high elevation pass at Wettzell are shown in Fig. 10.

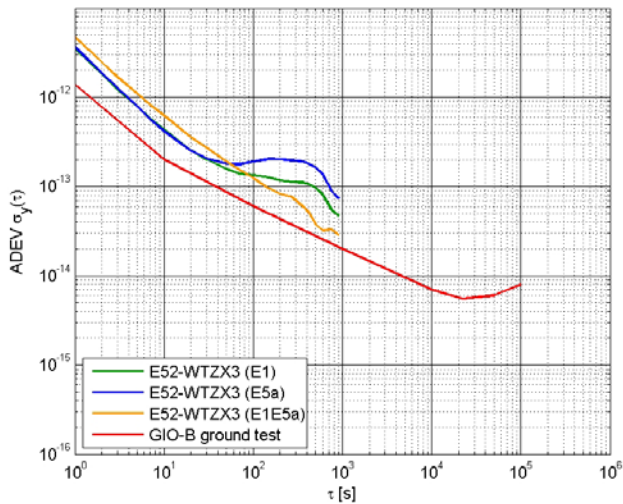


Fig. 10 Allan deviation of the GIOVE-B (PRN E52) Passive Hydrogen Maser from short-arc analysis of one-way carrier phase observations at the Wettzell CONGO station on Dec 4, 2010 (DOY 339).

Below 10 s, a τ^{-1} dependency of the Allan deviation is obtained which indicates white phase noise as the dominating contribution to the apparent clock variance. Similar to the analysis of the G25 measurements (cf. Fig. 7) the single frequency (E1 or E5a) processing yields a more favorable variance than the use of E1/E5a dual-

frequency carrier phase measurements at short time intervals. However, the single-frequency processing degrades already at $\tau \sim 30$ s as a result of increased ionospheric path delay variations. Overall, the variance of the GIOVE-B PHM derived from the one-way carrier phase analysis exceeds the ground test results by a factor of 2-3 over time scales of 1-100 s.

Comparison

To facilitate a direct comparison of both clocks, representative Allan deviation measurements of the GIOVE-B PHM and Block IIF-1 RFS from Figs. 2, 6-7, and 9-10 have been merged into a single graph shown in Fig. 11.

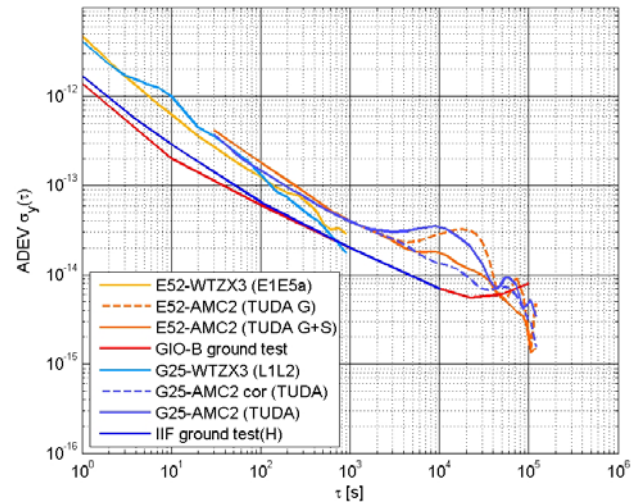


Fig. 11 Allan deviation of the GIOVE-B (PRN E52) Passive Hydrogen Maser and the Block IIF-1 (PRN G25) Rubidium Frequency Standard in comparison with ground performance measurements.

Overall, both clocks exhibit an excellent stability and the performance of the apparent clocks is only a factor of 2-3 worse than the performance of the respective oscillators measured in life tests on ground. Despite a widely different design, both clocks exhibit a strikingly similar performance up to correlation time scales of about 2,000 s. Differences between the ADEV of both clocks in this domain are generally small and can be understood by differences in the measurement equipment (receiver noise and multipath, number of stations in the monitoring network, etc.).

At longer time scales the apparent clocks of both spacecraft are potentially affected by orbit periodic variations. These are well known to result in a “bump” of the measured Allan deviation at half the harmonic period and a sharp drop at the period itself [26]. Despite the apparent similarity of the ADEV bump for both spacecraft, important differences may be noted upon closer inspection. In case of Block IIF-1, the observed clock exhibits both 1/rev and 2/rev variations with a similar amplitude. Such variations may also be recognized in the analysis of a geometry- and ionosphere-free triple-

carrier combination, which provides strong evidence for thermally induced line bias variations as the root cause of the apparent clock variations. On the other hand, line bias variations cannot presently be separated from thermally induced frequency variations of the rubidium oscillator itself. Irrespective of their actual nature, the orbit periodic clock variations and their seasonal dependence can be described with adequate accuracy through an empirical model based on the instantaneous orbit angle and Sun-angle w.r.t. the orbital plane. The model-based correction results in a notable reduction of the ADEV bump for the IIF-1 satellite and can be used to improve the quality of predicted clock solutions over times scales of up to a day.

For GIOVE-B, variations of the apparent PHM clock are clearly dominated by 1/rev contributions, while 2/rev terms are of low relevance. A comparison of orbit and clock products based on different processing strategies, networks and analysis centers suggests that the GIOVE orbit determination is prone to once-per-rev orbit errors, which in turn map into associated clock variations. In addition, a high correlation between periodic clock variations and satellite laser ranging residuals can be identified for the individual GIOVE-B orbit-clock products. Finally, 1/rev terms in the clock solution are strongly suppressed, when processing both GNSS observations and SLR measurements in the orbit-clock determination process. These findings suggest that the ADEV bump in the apparent clock of GIOVE-B is mainly driven by orbit determination errors but is unrelated to the actual oscillator performance.

SUMMARY AND CONCLUSIONS

A comparison of observed clock variances for the GIOVE-B passive hydrogen maser and the GPS Block IIF-1 rubidium frequency standard has been performed. For time intervals of 10-1,000 s, the apparent clocks of both spacecraft exhibit an almost identical Allan deviation of roughly $2 \cdot 10^{-12} \tau^{-1/2}$. This is only 2-3 times worse than the oscillator performance measured in ground based laboratory tests and marks a notable progress compared to previously available onboard frequency standards. At orbital time scales, periodic variations have been encountered which currently limit the clock prediction at (sub-)daily time scales. In case of the GPS Block IIF-1 satellite thermal line bias variations appear as a likely cause of the apparent clock variations. For GIOVE-B, in contrast, the observed clock variations can essentially be attributed to orbit determination errors.

To fully exploit the high quality of the new frequency standards, at time scales of 10,000 s and beyond, further effort will be required. In case of the GIOVE (or future Galileo) satellites, the rapid deployment of a sufficiently dense monitoring station network appears mandatory to achieve a high quality orbit determination. In particular, the possibility to perform ambiguity-fixed solutions appears as an important means for improving the quality of GIOVE-B GNSS-only ephemerides. With respect to

the GPS Block IIF satellites, a thorough inspection and analysis of the onboard equipment would be required to identify and, potentially mitigate, the observed thermal sensitivity of the overall radio-frequency chain. However, modifications of the current design appear highly unlikely at present, since the current signal and navigation performance is very well within the mission specification. Limited progress for advanced users can, nevertheless, be made through a careful monitoring of the clock variations and an empirical adjustment of harmonic model functions. A preliminary model of this form has been developed and presented for the IIF-1 satellite, but its general validity can only be assessed once further Block IIF satellites become operational.

ACKNOWLEDGEMENTS

Precise GPS ephemerides and clock solutions for use within this study have been obtained from the Center for Orbit Determination in Europe (CODE) at the Astronomical Institute of the University of Bern (AIUB). Satellite laser ranging measurements of GIOVE-B were, furthermore, provided by the International Laser Ranging Service (ILRS). The support of the above institutions is gratefully acknowledged. Triple-frequency observations of the Block IIF-1 GPS satellite and E1/E5 observations of GIOVE-B have been provided by the CONGO multi-GNSS network. The contributions of all network partners (Deutsches Zentrum für Luft- und Raumfahrt, Bundesamt für Kartographie und Geodäsie, Technische Universität München, Deutsches GeoForschungsZentrum, Centre National d'Etudes Spatiales, Geoscience Australia) and local station hosts are likewise gratefully acknowledged.

REFERENCES

- [1] Warren D.L.M., Raquet J.F.; "Broadcast vs. Precise GPS Ephemerides: a Historical Perspective"; *GPS Solutions*, 7:151–156 (2003).
- [2] Taylor J., Barnes E.; "GPS Current Signal-in-Space Navigation Performance"; *Proc. ION-NTM-2005*, 24-26 Jan 2005, San Diego; pp. 385-393 (2005).
- [3] Cohenour C., van Graas F.; "GPS Orbit and Clock Error Distributions"; *NAVIGATION: Journal of The Institute of Navigation*, 58(1):17-28 (2011).
- [4] Ostillo A., Johansson M., Hannes D., Malik M., Rest A., Waller P., Belloni M., Droz F., Mosset P.; "Passive Hydrogen Maser (PHM): the heart of the Galileo navigation payload"; *ENC-GNSS 2009*, 3-6 May 2009, Naples, Italy (2009).
- [5] Dupuis R.T., Lynch T.J., Vaccaro J.R., Watts E.T.; "Rubidium Frequency Standard for the GPS IIF Program and Modifications for the RAFSMOD Program"; *ION-GNSS-2010*, 21-24 Sep. 2010, Portland, OR (2010).
- [6] Waller P., Gonzalez F., Binda S., Sesia I., Tavella P., Hidalgo I., Tobias G.; "Update on the In-orbit Performances of GIOVE Clocks"; *Proceedings EFTF 2009*, 388-392 (2009).

- [7] Droz F., Mosset P., Wang Q., Rochat P., Belloni M., Gioia M., Rest A., Waller P.; "Space Passive Hydrogen Maser - Performances and Lifetime Data"; Proceedings EFTF 2009, 393-398 (2009).
- [8] Waller P.; Gonzalez F., Binda S., Rodriguez D., Tobias G., Cernigliaro A., Sesia I., Tavella P.; Proc. 42nd Annual Precise Time and Time Interval (PTTI) Meeting, 15-18 Nov. 2010, Reston VA; pp. 171-179 (2010).
- [9] Vannicola F., Beard R., White J., Senior K., Kubik A., Wilson D.; "GPS Block IIF Rubidium Frequency Standard Life Test"; ION-GNSS-2010, 21-24 Sep. 2010, Portland, OR (2010).
- [10] Vannicola F., Beard R., White J., Senior K., Largay M., Buisson J.; "GPS Block IIF Atomic Frequency Standard Analysis"; Proc. 42nd Annual Precise Time and Time Interval (PTTI) Meeting, 15-18 Nov. 2010, Reston VA; 181-196 (2010).
- [11] Senior K.; "SVN62 Clock Analysis using IGS Data", IGSMAIL-6218, 6 Aug 2010, (2010). <http://igs.cb.jpl.nasa.gov/pipermail/igsmail/2010/000051.html>
- [12] Montenbruck O., Hauschild A., Steigenberger P., Langley R.B. "Three's the Challenge: A Close Look at GPS SVN62 Triple-frequency Signal Combinations Finds Carrier-phase Variations on the New L5", GPS World 21(8):8-19 (2010).
- [13] Dow J.M., Neilan R.E., Rizos C.; "The International GNSS Service in a changing landscape of Global Navigation Satellite Systems", Journal of Geodesy 83(3-4):191-198 (2009). DOI 10.1007/s00190-008-0300-3
- [14] Montenbruck O., Hauschild A., Hessels U.; "Characterization of GPS/GIOVE Sensor Stations in the CONGO Network"; GPS Solutions 15(3), 193-205 (2011). DOI 10.1007/s10291-010-0182-8
- [15] Pearlman, M.R., Degnan, J.J., and Bosworth, J.M., "The International Laser Ranging Service", Advances in Space Research, 30(2):135-143 (2002). DOI:10.1016/S0273-1177(02)00277-6
- [16] Dach R., Brockmann E., Schaer S., Beutler G., Meindl M., Prange L., Bock H., Jäggi A., Ostini L.; "GNSS processing at CODE: status report", Journal of Geodesy 83(3-4):353-365 (2009). DOI 10.1007/s00190-008-0281-2
- [17] Griffiths J., Ray J.R.; "On the precision and accuracy of IGS orbits", Journal of Geodesy 83(3-4):277-287 (2009). DOI 10.1007/s00190-008-0237-6
- [18] Montenbruck O., Hugentobler U., Dach R., Steigenberger P., Hauschild A.; "Apparent Clock Variations of the Block IIF-1 (SVN62) GPS Satellite"; GPS Solutions (2011). DOI 10.1007/s10291-011-0232-x
- [19] Steigenberger P., Hugentobler U., Montenbruck O., Hauschild A.; "Precise Orbit Determination of GIOVE-B Based on the CONGO Network"; Journal of Geodesy 85(6):357-365 (2011). DOI 10.1007/s00190-011-0443-5
- [20] Svehla D., Heinze M., Rothacher M., Steigenberger P., Dähnn M., Kirchner M.; "Combined processing of GIOVE-A and GPS measurements using zero- and double-differences". Geophys Res Abstr 10. sRef-ID: 1607-7962/gra/EGU2008-A-11383 (2008).
- [21] Springer T.; Dow J.; Sanchez J. F.; Romero I.; "Combined processing of observations from different Global Navigation Satellite Systems"; #G11A-07; American Geophysical Union, Fall Meeting 2007, San Francisco (2007).
- [22] Kouba J.; "Improved Relativistic Clock Correction due to Earth Oblateness", GPS Solutions 8(3):170-180 (2004). DOI 10.1007/s10291-004-0102-x
- [23] Bock H., Dach R., Jäggi A., Beutler B. "High-rate GPS clock corrections from CODE: support of 1 Hz applications"; Journal of Geodesy 83(11):1083-1094 (2009). DOI 10.1007/s00190-009-0326-1
- [24] Gonzalez F., Waller P.; "Short-term GNSS Clock Characterization using One-Way Carrier Phase"; IEEE 07CH37839; Proc. IEEE Int. Freq. Control Symp. & 21st European Freq. and Time Forum (EFTF), 29 May - 1 June 2007, Geneva, Switzerland, pp. 517-522 (2007). DOI 10.1109/FREQ.2007.4319127
- [25] Delporte J., Boulanger C., Mercier F.; "Simple Methods for the Estimation of the Short-Term Stability of GNSS On-Board Clocks"; Proc. 42nd Annual Precise Time and Time Interval (PTTI) Meeting, 15-18 Nov. 2010, Reston VA; pp. 215-224 (2010).
- [26] Riley WR (2008) Handbook of Frequency Stability Analysis, NIST Special Publication 1065, National Institute of Standards and Technology, Boulder CO
- [27] Hugentobler U., Steigenberger P., Montenbruck O., Hauschild A., Weber G., Hessels U.; "Evaluation of GIOVE Satellite Clocks using the CONGO Network", 24th European Frequency and Time Forum, 13-16 April 2010, Noordwijk, The Netherlands (2010).
- [28] Zandbergen R., Navarro D.; "Specification of Galileo and GIOVE space segment properties relevant for Satellite Laser Ranging"; ESA-EUING-TN/10206, rev. 3.2, 8 May 2008; European Space Agency (2009).
- [29] Svehla D., Schönemann E., Escobar D., Springer T.; "Complete Relativistic Modelling of the GIOVE-B clock parameters and its impact on POD, track-track ambiguity resolution and precise timing", IGS Workshop, 2 July 2010, Newcastle, England, UK (2010).